Structural models for the $\sqrt{19} \times \sqrt{19}$ reconstruction of the $GaAs(\bar{1}\bar{1}\bar{1})$ surface and their relative stabilities

Structural models for the $\sqrt{19} \times \sqrt{19}$ reconstruction of the GaAs($\bar{1}\bar{1}\bar{1}$) surface and their relative stabilities

M Haugk, J Elsner, M Sternberg and Th Frauenheim

Technische Universität, Institut für Physik, Theoretische Physik III, D-09107 Chemnitz, Germany

Abstract. We present a theoretical study of the relative formation energies for possible models of the $\sqrt{19} \times \sqrt{19}$ reconstruction found under Ga-rich growth conditions at the GaAs($\bar{1}\bar{1}\bar{1}$) surface. The energetically most favourable model has fourfold-coordinated Ga atoms on the surface, exhibiting metallic bonding character. This structure differs as regards the electron-counting rule (ECR) from the well accepted models for the (100), (110) and (111) surfaces of GaAs. Our results suggest that it is still possible to explain the stability of the metallic ($\bar{1}\bar{1}\bar{1}$) surface with a rule similar to the ECR.

1. Introduction

A lot of progress has been made during recent years in determining the geometries of semiconductor surface reconstructions. In particular, total-energy calculations have been used to suggest atomic models for the most important reconstructions of the GaAs(110) [1], GaAs(111) [2] and GaAs(100) [3] surfaces which are consistent with experimental data obtained by low-energy electron diffraction (LEED) [4] and scanning tunnelling microscopy (STM) [5].

A common feature of all of these energetically favourable models is that they obey the electron-counting rule (ECR). This rule demands the energetically high Ga-derived dangling bonds to be emptied in favour of filling the As-derived dangling bonds having energies close to the valence band maximum (VBM). The charge transfer is often accompanied by a rehybridization yielding sp^2- (p^3-) bonded Ga (As) atoms in order to reduce the surface energy and to make the surface semiconducting. This rule is a useful tool for the construction of energetically promising surface models. To explain the 2×2 periodicity observed at the GaAs($\bar{1}\bar{1}\bar{1}$) surface in an As-rich environment, the semiconducting As trimer model was suggested on the basis of the ECR as a possible candidate, which was then confirmed by total-energy calculations [6]. Unfortunately, the electron-counting rule cannot be used to predict any semiconducting model for the $\sqrt{19} \times \sqrt{19}$ periodicity reported in a Ga-rich environment [6–10]. Due to symmetry constraints this surface has to be metallic in its neutral charge state. Moreover, it is not clear whether energetically favourable metallic surfaces could be found or explained by a model as simple as the ECR. Several structures have already been suggested to explain the $\sqrt{19} \times \sqrt{19}$ periodicity [6, 11]. However, a total-energy calculation by means of standard SCF-LDA schemes is still computationally too expensive.

In this paper we present calculations for the formation energies of various new models for the GaAs($\bar{1}\bar{1}\bar{1}$) $\sqrt{19} \times \sqrt{19}$ reconstruction together with previously examined models

for 2×2 reconstructions [6, 11] using a self-consistent charge-density-functional-based tight-binding (*SCC-DFTB*) approach [12].

In section 2 we briefly describe the calculational details. We present our results in section 3. Finally we give a summary in section 4.

2. Theory

2.1. Method

For our calculations we use a recently developed self-consistent-charge extension of the density-functional-based tight-binding methodology [12]. The method differs from previous approaches since the modification of the TB total-energy expression is based on a second-order expansion of the *Kohn–Sham* energy functional [13] with respect to density fluctuations. Following Foulkes and Haydock [14], a superposition of a reference or input density $n_0' = n_0(r')$ and a small fluctuation $\delta n' = \delta n(r')$ is substituted for the charge density in the Kohn–Sham energy functional. In rewriting the total energy, they transform the leading (*zeroth-order*) matrix elements and derive an energy functional that is correct to *second-order* terms in the charge fluctuations:

$$E = \sum_{i}^{\text{occ}} \langle \Psi_i | \hat{H}_0 | \Psi_i \rangle - \frac{1}{2} \int \int \frac{n_0' n_0}{|r - r'|} \, dr \, dr' + E_{\text{xc}}[n_0] - \int V_{\text{xc}}[n_0] n_0 \, dr + E_{ii}$$
$$+ \frac{1}{2} \int \int \left(\frac{1}{|r - r'|} + \frac{\delta^2 E_{\text{xc}}}{\delta n \, \delta n'} \bigg|_{n_0} \right) dr \, dr' \, \delta n \, \delta n'. \tag{1}$$

Furthermore, in reference [12] it was shown that by approximating the charge fluctuations $\delta n(r)$ by spherical contributions centred at the atomic sites, the DFT total energy can be rewritten in a transparent tight-binding form:

$$E = \sum_{i}^{\text{occ}} \langle \Psi_i | \hat{H}_0 | \Psi_i \rangle + E_{\text{rep}}[n_0] + \frac{1}{2} \sum_{\alpha, \beta}^{N} \gamma_{\alpha\beta} \, \Delta q_\alpha \, \Delta q_\beta. \tag{2}$$

The first sum runs over occupied Kohn–Sham eigenstates Ψ_i with the Hamilton operator resulting from the input density $n_0(r)$. The second term is a pairwise, short-range repulsive potential including the core–core repulsion E_{ii} and the double-counting Hartree and XC contributions in (1) which depend on the input density n_0 [14]. Finally, the last sum is taken over all atoms of the system and accounts for the second-order corrections of the total energy due to fluctuations in the charge density. In our scheme the total charge fluctuation at atom α (Δq_α) is evaluated in the Mulliken analysis. $\gamma_{\alpha\beta}$ represents the functional

$$\gamma_{\alpha\beta} = \int \int \left(\frac{1}{|r - r'|} + \frac{\delta^2 E_{\text{xc}}}{\delta n \, \delta n'} \bigg|_{n_0} \right) n_\alpha(|r' - R_\alpha|) n_\beta(|r - R_\beta|) \, dr \, dr' \tag{3}$$

with $n_\alpha(|r - R_\alpha|)$ as the spherical charge distribution centred at atom α. This functional yields the pure Coulomb interaction between two charge distributions at R_α, R_β in the limit of large distance. For $\alpha = \beta$ the functional $\gamma_{\alpha\beta}$ gives the self-interaction contribution of atom α. To evaluate the integral it is necessary to expand the charge densities in an appropriate basis for which we choose Slater-type functions.

By using the variational technique for minimizing the approximate energy expression (2) within the LCAO framework, in reference [12] generalized Hamiltonian matrix elements are derived. These, compared with those in the standard TB approach, are modified by the

self-consistent redistribution of *Mulliken* charges:

$$\sum_{v}^{M} c_{vi}(H_{\mu v} - \varepsilon_i S_{\mu v}) = 0 \qquad \forall \mu, i \qquad (4)$$

$$H_{\mu v} = \langle \varphi_\mu | \hat{H}_0 | \varphi_v \rangle + \frac{1}{2} S_{\mu v} \sum_{\xi}^{N} (\gamma_{\alpha\xi} + \gamma_{\beta\xi}) \Delta q_\xi \qquad S_{\mu v} = \langle \varphi_\mu | \varphi_v \rangle \qquad \forall \mu \in \alpha, v \in \beta.$$

$$(5)$$

This method involves performing total-energy calculations with an accuracy comparable to that of SCF-LDA calculations. In contrast to these computationally expensive schemes, the SCC-DFTB method can be used for structures containing several hundred atoms. Applied to the (110), (111) and (100) surfaces of GaAs, the SCC-DFTB scheme gave geometries and absolute surface energies [12, 15] which are in very good agreement with the SCF-LDA calculations carried out by Moll *et al* [16].
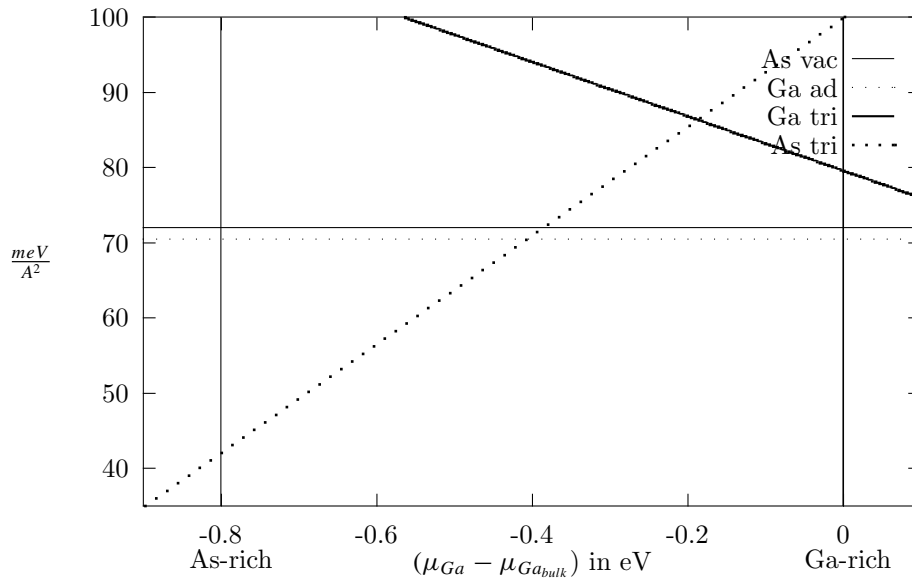

Figure 1. Surface energies of GaAs($\bar{1}\bar{1}\bar{1}$) structures with 2×2 periodicity plotted versus the Ga chemical potential. The part on the left (right) of the diagram corresponds to As- (Ga-) rich growth conditions.

2.2. Details of the calculation and analysis

The ($\bar{1}\bar{1}\bar{1}$) surfaces were modelled by slabs each consisting of ten monolayers with periodic boundary conditions in two dimensions. The first six monolayers were allowed to relax, while the remaining atoms were fixed to preserve the bulk lattice spacing. In order to prevent artificial charge transfer between the bottom of the slab and the surface, we saturated the Ga dangling bonds at the bottom with pseudo-hydrogen having a charge of 1.25 *e*. This charge corresponds to the charge per bond contributed from a tetrahedrally bound As atom [17]. Four (two) *k*-points were used to sample the Brillouin zone of the supercell with 2×2 ($\sqrt{19} \times \sqrt{19}$) periodicity. Numerical tests have shown that our models converge with respect to the number of *k*-points employed and the slab thickness.

The relative stabilities of two structures having different numbers of Ga and As atoms depend on the reservoir with which the atoms are exchanged in the structural transition. Questions of thermodynamic stability are therefore posed within the context of atomic chemical potentials [18]. It can be shown that the surface energy can be expressed as a function of the atomic chemical potential of one species, which we take to be μ_{Ga}:

$$\gamma_0 = [E_{\text{tot}} - \mu_{\text{GaAs}}^{\text{cryst}} N_{\text{As}} - \mu_{\text{Ga}}(N_{\text{Ga}} - N_{\text{As}})]/F \tag{6}$$

where F denotes the area of the surface cell and $N_{\text{As (Ga)}}$ the total number of As (Ga) atoms. The allowed range of this chemical potential is then

$$\mu_{\text{Ga(bulk)}} - \Delta H_f \leqslant \mu_{\text{Ga}} \leqslant \mu_{\text{Ga(bulk)}}$$

ranging from the As-rich ($\mu_{\text{Ga}} = \mu_{\text{Ga(bulk)}} - \Delta H_f$) to the Ga-rich ($\mu_{\text{Ga}} = \mu_{\text{Ga(bulk)}}$) environment. ΔH_f is the heat of formation for GaAs, which has been determined from enthalpy measurements to be 0.74 eV [19]. To obtain absolute surface energies we use an energy-density formalism [20] in a modified version for TB [15].
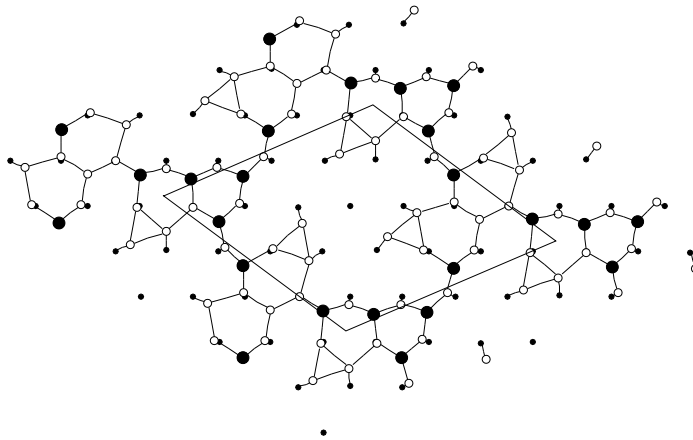

Figure 2. The top view of the Ga trimer model. Large (small) filled circles represent top- (third-) layer As atoms; empty circles represent second-layer Ga atoms.

3. Results

We first investigate the most stable surfaces with 2×2 periodicity, the As vacancy, the Ga adatom and the Ga and As trimer models. For illustrations of these structures see reference [16]. The absolute surface energies depending on the Ga chemical potential obtained with the SCC-DFTB scheme are shown in figure 1. The values are very similar to those calculated by Moll *et al* [16] and can be compared to the relative formation energies of Biegelsen *et al* [6]. In agreement with those studies, we find the As trimer to be by far the most stable structure under As-rich growth conditions, whereas the Ga trimer has very high surface energy in any environment.

We now turn to models with $\sqrt{19} \times \sqrt{19}$ periodicity. This type of reconstruction can be observed by heating [7, 8] or annealing [6] the sample at about 500 °C. A significant desorption of surface As is reported at the transition from 2×2 to $\sqrt{19} \times \sqrt{19}$ periodicity. Moreover, Woolf *et al* [9] found that the $\sqrt{19} \times \sqrt{19}$ periodicity does not exist under a

Table 1. The bonding configuration of the first-layer As atoms.

Surface	First-layer As	Coordination	Hybridization
Ga twofold	6	6×3	p^3
Ga trimer	6	6×3	p^3
Ga metallic	6	6×3	p^3

Table 2. The bonding configuration of the second-layer Ga atoms.

Surface	Second-layer Ga	Coordination	Hybridization
Ga twofold	12	6×3	sp^2
		4×3	Linear Ga–Ga–As
		2×2	$155°$
Ga trimer	19	7×3	sp^2
		3×3	Distorted p^3
		6×4	Metallic bonding character
		3×4	sp^3
Ga metallic	18	15×3	sp^2
		3×4	Metallic bonding character

Table 3. The bonding configuration of the third-layer As atoms.

Surface	Third-layer As	Coordination	Hybridization
Ga twofold	19	7×3	sp^3
		12×4	sp^3
Ga trimer	19	1×3	sp^3
		18×4	Distorted sp^3
Ga metallic	19	4×3	sp^3
		15×4	sp^3

strong As_4 flux. These results clearly show that the $\sqrt{19} \times \sqrt{19}$ surface should exist in a Ga-rich environment.

Kaxiras *et al* [11] suggested a model consisting of Ga trimers and threefold-coordinated As atoms at the surface. If one counts all As and Ga dangling bonds in this structure (see reference [11] for a figure), all As lone pairs can be filled, leaving $\frac{3}{4}$ of an electron to be placed into Ga-derived dangling bonds. These, however, have high energies, causing the structure to relax from this configuration. The resulting geometry is shown in figure 2. Tables 1, 2 and 3 give the total number of atoms, the coordination numbers and the hybridization types of the atoms for the first-layer As, second-layer Ga and third-layer As atoms. Analysing the bonding configuration of this specific surface, it is possible to describe its stability in a manner that is similar to the ECR. In contrast to semiconducting surfaces, there are fourfold-coordinated Ga atoms which are not in a typical sp^n-hybridization state. They are therefore considered to exhibit metallic Ga bonding character like in the bulk Ga crystal. Hence, the electrons could be distributed in such a way that all As dangling bonds are filled, all Ga dangling bonds are emptied and excess charge is placed in the Ga bonds with metallic character. However, the surface energy is high—see figure 3—predicting this
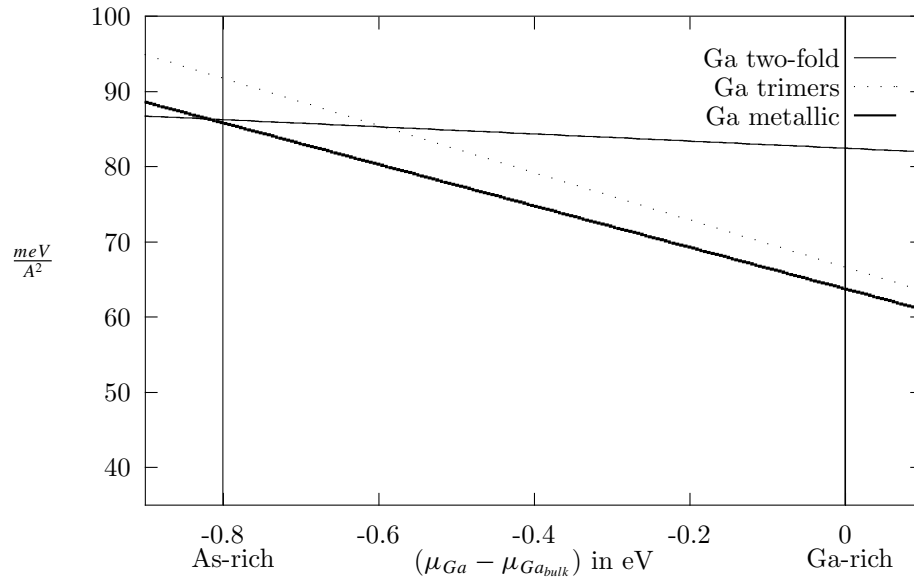
Figure 3. Surface energies plotted versus the Ga chemical potential of various models for the $\sqrt{19} \times \sqrt{19}$ GaAs($\bar{1}\bar{1}\bar{1}$) surface. The part on the left (right) of the diagram corresponds to As-(Ga-) rich growth conditions.
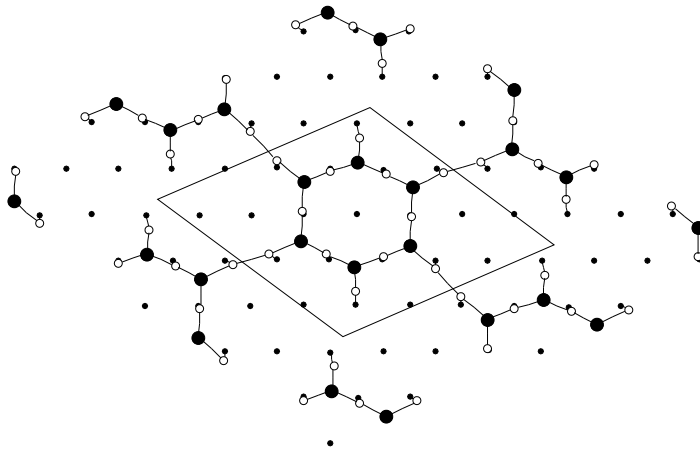

Figure 4. The top view of the Ga twofold model. Large (small) filled circles represent top-(third-) layer As atoms; empty circles represent second-layer Ga atoms.

model to be energetically unfavourable. This can be understood by noting that surface Ga trimers are far from being sp^2 coordinated and thus have a high surface energy; see figure 1.

High-resolution STM images obtained by Biegelsen *et al* [6] furthermore indicate that the top-layer As atoms should be arranged within a hexagonal ring. To match the STM images, Biegelsen *et al* proposed a model in which six top-layer As atoms are bound to six threefold- and six twofold-coordinated Ga atoms. A figure showing the structure before the geometrical optimization was performed can be found in reference [6]. Again, all As lone pairs are filled. Due to the six twofold-coordinated Ga atoms, 3.75 electrons would

have to occupy Ga-derived dangling bonds. It is therefore not surprising that the atoms relax towards a configuration with only two twofold-coordinated Ga atoms and yielding four additional Ga–Ga bonds; cf. figure 4. The Ga–Ga bonding is achieved by forcing the Ga atoms into nearly linear Ga–Ga–As chains (see table 2), which are energetically costly. The resulting high surface energy, shown in figure 3, suggests that this model does not correspond to the observed STM picture.
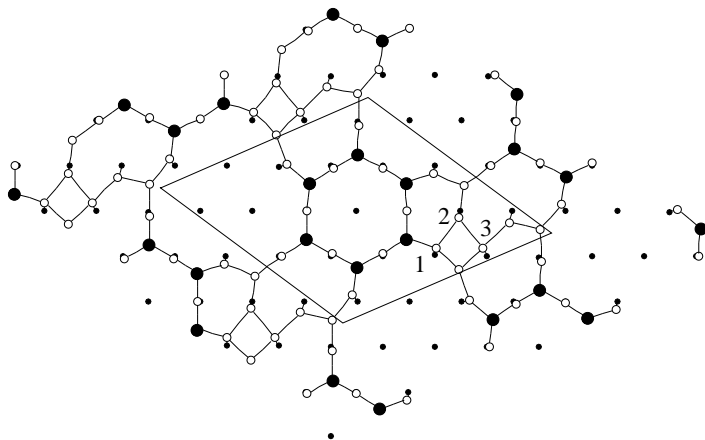

Figure 5. The top view of the Ga metallic model. Large (small) filled circles represent top- (third-) layer As atoms; empty circles represent second-layer Ga atoms.
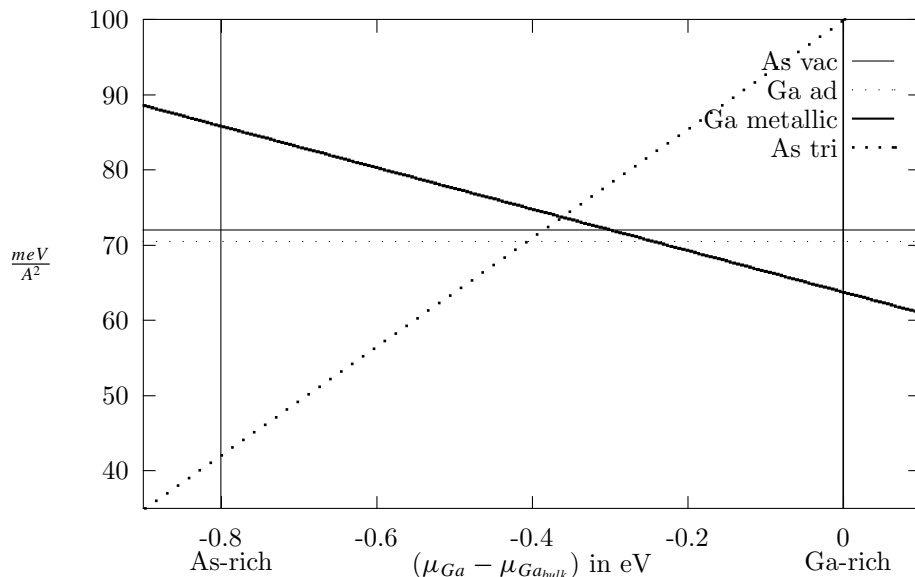

Figure 6. Surface energies of the GaAs($\bar{1}\bar{1}\bar{1}$) structures plotted versus the Ga chemical potential. The part on the left (right) of the diagram corresponds to As- (Ga-) rich growth conditions.

We then investigated the stability of a variety of different structures with preferably threefold-coordinated Ga and As surface atoms. However, we found high surface energies

Table 4. Distances ($\overline{\Delta z}$) in Å between the first three layers.

Surface	First-layer As to second-layer Ga	Second-layer Ga to third-layer As
Ga twofold	0.95	2.25
Ga trimer	0.99	2.43
Ga metallic	0.74	2.51
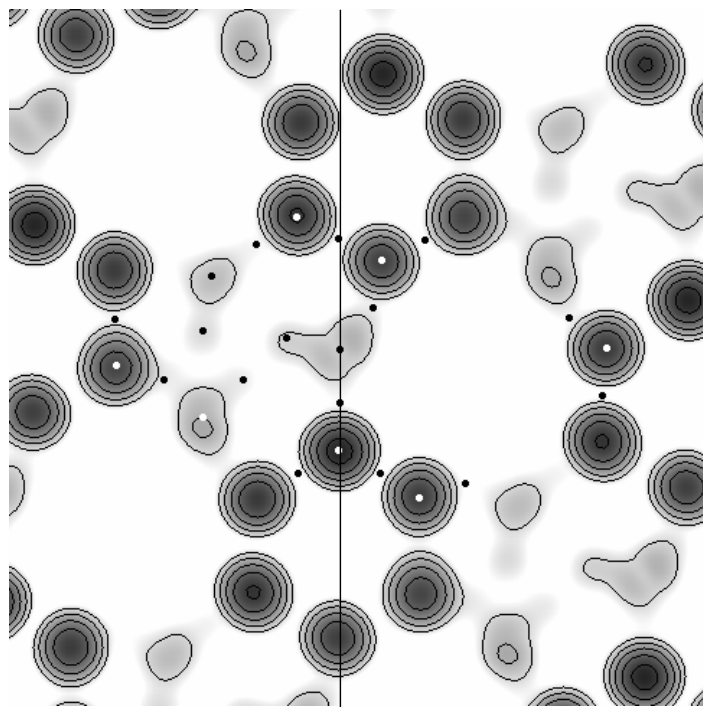
Figure 7. A horizontal plot of the charge density within a 1 Å distance from the surface atoms for an energy of 1.8 ± 0.1 eV. Black and white dots mark the atom positions in the first two layers. The black line indicates the position of the vertical cut.

for all of these structures. We then constructed models where Ga–Ga bonds could form, favouring fourfold-coordinated Ga atoms. The energetically most auspicious configuration obtained is shown in figure 5. In agreement with the previously discussed model, suggested on the basis of STM pictures given by Biegelsen *et al* [6], six top-layer As atoms form a hexagonal ring. They all adopt p^3 hybridization with doubly occupied s-like orbitals; see table 1. Fifteen threefold-coordinated and three fourfold-coordinated Ga atoms build the second layer; cf. table 2. The threefold-coordinated Ga atoms move to an sp^2-like hybridization. But the most important feature is the existence of the three fourfold-coordinated Ga atoms, labelled 1, 2, 3 in figure 5. These Ga atoms exhibit weak metallic Ga–Ga bonds with a bond length of ≈ 2.9 Å which is slightly larger than that in bulk Ga (≈ 2.7 Å). As discussed for the Ga metallic bonds in the $\sqrt{19} \times \sqrt{19}$ Ga trimer model proposed by Kaxiras *et al* [11], this structure allows the non-ECR-compensated excess charge to be placed into Ga–Ga bonds before Ga-derived dangling bonds would have to be

occupied. All As lone pairs are filled. Therefore, as for the $\sqrt{19} \times \sqrt{19}$ Ga trimer structure, a rule similar to the ECR may be used to explain the stability of this surface configuration. Hence, this rule can be called a modified electron-counting rule. Additional to the obeying of the modified ECR, we found another feature that favours this surface being more stable than the other ones. All surface Ga atoms are either sp^2 hybridized (threefold coordinated) or exhibit metallic bonding character (fourfold coordinated) and consequently do not have to adopt energetically unfavourable configurations, like the Ga trimer or the Ga–Ga–As linear chain structures. These two facts explain why the formation energy of this structure is low; see figure 3. It is worth noting that reconstructions of polar GaN surfaces, where metallic Ga is believed to be at the surface, could be driven by a similar mechanism.

Finally, figure 6 shows the energies of the most stable 2×2 reconstructions together with the proposed model for the $\sqrt{19} \times \sqrt{19}$ surface. We see that the proposed model is energetically favourable under Ga-rich growth conditions and could thus be a candidate for explaining the observed periodicity. The interlayer distances, which could be useful for further STM investigations, are listed in table 4.

Figure 8. A vertical plot of the charge density. The black line marks the plane of the horizontal cut.

Analysing the structure in figure 5, one might expect the Ga metallic bonds in the most stable structure to become a remarkable feature appearing in an STM experiment. We therefore calculated the charge density within an energy range of 1.8 ± 0.1 eV below the Fermi level at 1 Å above the surface atoms (figure 7) and in a vertical cut (figure 8) along a line marked in figure 7. The density is plotted over a range of four orders of magnitude, from dark regions with high charge density to white regions with almost no charge density. It can clearly be seen that the As hexagonal ring is the dominant feature which was identified in the STM measurements of Biegelsen *et al* [6]. The influence of the Ga metallic bonds in the charge-density distribution is very small compared to that of the dominant markers arising from the As lone pairs. The symmetry of the As hexagon is not disturbed significantly.

4. Summary

Summarizing our results, we suggest a model for the $\sqrt{19} \times \sqrt{19}$ reconstruction of the GaAs($\bar{1}\bar{1}\bar{1}$) surface which is energetically favourable under Ga-rich growth conditions. The atomic geometry is consistent with STM data. The structure has all As (Ga) lone pairs (dangling bonds) filled (emptied) and partially filled metallic Ga–Ga bonds. We conclude that metallic surfaces which obey a modified electron-counting rule where all As (Ga) dangling bonds are filled (emptied) and excess charge is placed into Ga metallic bonds might have low surface energies in compound semiconductors.

Acknowledgments

References

[1] Qian G-X, Martin R M and Chadi D J 1988 *Phys. Rev.* B **37** 1303
[2] Kaxiras E, Bar-Yam Y, Joannopoulos J D and Pandey K C 1987 *Phys. Rev.* B **35** 9625
[3] Northrup J E and Froyen S 1994 *Phys. Rev.* B **50** 2015
[4] Tong S Y, Xu G and Mei W N 1984 *Phys. Rev. Lett.* **52** 1693
[5] Hashizume T, Xue Q K, Zhou J, Ichimiya A and Sakurai T 1995 *Phys. Rev. Lett.* **74** 3177
[6] Biegelsen D K, Bringans R D, Northrup J E and Schwartz L E 1990 *Phys. Rev. Lett.* **65** 452
[7] Cho A Y and Hayashi I 1971 *Solid-State Electron.* **14** 125
[8] Arthur R 1974 *Surf. Sci.* **43** 449
[9] Woolf D A, Westwood D I and Williams R H 1993 *Appl. Phys. Lett.* **62** 1371
[10] Ren Hong-Wen and Nishinaga T 1996 *Phys. Rev.* B **54** R11 054
[11] Kaxiras E, Bar-Yam Y, Joannopoulos J D and Pandey K C 1987 *Phys. Rev.* B **35** 9636
[12] Elstner M, Porezag D, Jungnickel G, Elsner J, Haugk M, Frauenheim Th, Suhai S and Seifert G 1998 *Phys. Rev.* B submitted
[13] Kohn W and Sham L J 1965 *Phys. Rev.* **140** A1133
[14] Foulkes W and Haydock R 1989 *Phys. Rev.* B **39** 12 520
[15] Haugk M, Elsner J and Frauenheim Th 1997 *J. Phys.: Condens. Matter* **9** 7305
[16] Moll N, Kley A, Pehlke E and Scheffler M 1996 *Phys. Rev.* B **54** 8844
[17] Shiraishi K 1990 *J. Phys. Soc. Japan* **59** 3455
[18] Qian G-X, Martin R M and Chadi D J 1988 *Phys. Rev.* B **38** 7649
[19] *CRC Handbook of Chemistry and Physics* 1986 67th edn, ed R C Weast (Boca Raton, FL: Chemical Rubber Company Press)
[20] Chetty N and Martin R M 1992 *Phys. Rev.* B **45** 6074